HHS Public Access

Author manuscript

Mol Microbiol. Author manuscript; available in PMC 2020 December 01.

Published in final edited form as:

Mol Microbiol. 2019 December ; 112(6): 1701–1717. doi:10.1111/mmi.14384.

The Loz1 transcription factor from *Schizosaccharomyces pombe* binds to Loz1 Response Elements and represses gene expression when zinc is in excess

Stevin Wilson[1], **Yi-Hsuan Liu**[2], **Carlos Cardona-Soto**[2], **Vibhuti Wadhwa**[3], **Mark P. Foster**[3,4], **Amanda J. Bird**[1,2,4,*]

[1]Department of Molecular Genetics, The Ohio State University, Columbus, OH, 43210

[2]Department of Human Nutrition, The Ohio State University, Columbus, OH, 43210

[3]Department of Chemistry and Biochemistry, The Ohio State University, Columbus, OH, 43210

[4]Center for RNA Biology, The Ohio State University, Columbus, OH, 43210

Summary

In *Schizosaccharomyces pombe* the expression of the *zrt1* zinc uptake gene is tightly regulated by zinc status. When intracellular zinc levels are low, *zrt1* is highly expressed. However, when zinc levels are high, transcription of *zrt1* is blocked in a manner that is dependent upon the transcription factor Loz1. To gain additional insight into the mechanism by which Loz1 inhibits gene expression in high zinc we used RNA-seq to identify Loz1-regulated genes, and ChIP-seq to analyze the recruitment of Loz1 to target gene promoters. We find that Loz1 is recruited to the promoters of 27 genes that are also repressed in high zinc in a Loz1-dependent manner. We also find that the recruitment of Loz1 to the majority of target gene promoters is dependent upon zinc and the motif 5'-CGN(A/C)GATCNTY-3', which we have named the Loz1 Response Element (LRE). Using reporter assays we show that LREs are both required and sufficient for Loz1-mediated gene repression, and that the level of gene repression is dependent upon the number and sequence of LREs. Our results elucidate the Loz1 regulon in fission yeast and provide new insight into how eukaryotic cells are able to respond to changes in zinc availability in the environment.

Abbreviated Summary

*To whom the correspondence should be addressed: Amanda J. Bird, Department of Human Sciences and Department of Molecular Genetics, The Ohio State University, 1787 Neil Avenue, Columbus, OH, 43210, Tel.: (614) 247 1559; Fax (614) 292 8880; bird.96@osu.edu.

Author's Contributions

M.P.F., and A.J.B., conceived the project, S.W., M.P.F., and A.J.B., designed the study, S.W. Y-H. L., C.C.S., V.W., A.J.B., performed the experiments, all authors conducted data analysis and S.W., C.C.S., V.W., M.P.F., A.J.B., contributed to manuscript editing.

Conflict of Interest

The authors declare that they have no conflicts of interest with the contents of this article.

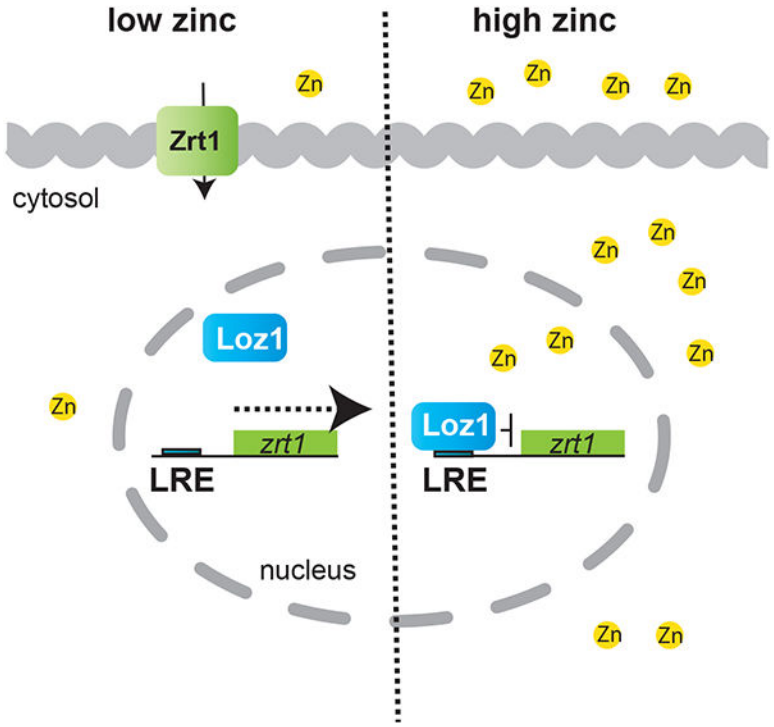

In fission yeast the transcription factor Loz1 plays a central role in zinc homeostasis by inhibiting gene expression when zinc is in excess. Here we show that Loz1 DNA binding activity is dependent upon cellular zinc status and that Loz1 binds in a site-specific manner to Loz1 Response Elements (LREs) that are located in target genes promoters. These studies provide new mechanistic insight into Loz1 function, and highlight new pathways that are regulated by zinc.

Keywords

DNA binding; metallo-regulatory; zinc finger; nutrient homeostasis; zinc transporter

Introduction

A diverse array of proteins require zinc for their function, including transcription factors containing C_2H_2-type zinc finger domains, and many enzymes that are required for basic cellular processes including: DNA replication, transcription, translation, and respiration (Andreini *et al.*, 2009, Coleman, 1992). As zinc ions can also be toxic in excess, cells require homeostasis mechanisms to maintain sufficient levels of zinc for incorporation into newly synthesized zinc proteins and at the same time do not inhibit growth (Bird, 2015). The importance of these zinc homeostasis mechanisms is underscored by the fact that multiple genetic diseases can result from zinc deficiency or imbalances in zinc ion levels including: *Acrodermatitis enteropathica*; transient neonatal zinc deficiency; early onset agammaglobulinemia; and the spondylocheirodysplastic form of Ehlers-Danlos syndrome (Wang *et al.*, 2004, Jeong *et al.*, 2012, Chowanadisai *et al.*, 2006, Anzilotti *et al.*, 2019).

The budding yeast *Saccharomyces cerevisiae* has been an important model system for deciphering mechanisms of cellular zinc homeostasis. In this yeast the transcription factor Zap1 plays a key role in the zinc starvation response by controlling the expression of genes required for zinc acquisition (*ZRT1*, *ZRT2*, and *FET4*) and the release of zinc from intracellular stores (*ZRT3*) (Eide, 2009, Wilson & Bird, 2016). When zinc levels are low, Zap1 binds to zinc responsive elements (ZREs) that are located within the promoters of these genes, increasing gene expression. In contrast, when zinc levels are high, Zap1 loses its ability to bind to DNA and to activate gene expression. Zap1 also controls how cells allocate zinc by regulating the expression of *ZRR1* and *ZRR2* - the non-coding RNAs that inhibit the expression of genes encoding alcohol dehydrogenase 1 and 3, respectively (Bird *et al.*, 2006). As alcohol dehydrogenases are abundant zinc-requiring proteins, the inhibition of *ADH1* and *ADH3* gene expression in low zinc helps cells to conserve zinc ions for more important functions.

In addition to having a primary role in zinc homeostasis, Zap1-dependent changes in gene expression alter cell metabolism so that they are able to survive longer periods of zinc starvation. Under these more severe conditions Zap1 induces the expression of additional genes that are required for stress resistance, cell wall function, and secretory pathway function (Wu *et al.*, 2008). Examples of these second-response genes include *TSA1*, which encodes a peroxiredoxin that has a dual role as a peroxidase and a holdase, and *ZRG17*, which encodes a CDF family member that is required for zinc transport from the cytoplasm into the endoplasmic reticulum (Wu *et al.*, 2007, Wu *et al.*, 2011). Further analyses of these genes and their protein products have shown that the holdase function of Tsa1 is critical for survival during severe zinc starvation, and that in the absence of the Zap1-dependent increase in *ZRG17* expression, cells experience increased protein unfolding in the endoplasmic reticulum (MacDiarmid *et al.*, 2013, Choi *et al.*, 2018). Studies of these Zap1 target genes therefore suggest that cells have programmed responses to counter stresses that arise from zinc starvation.

In the fission yeast *Schizosaccharomyces pombe* multiple zinc homeostasis genes are regulated at a transcriptional level in response to zinc status, including *zrt1* and *adh1* (Dainty *et al.*, 2008, Ehrensberger *et al.*, 2013). However, in this yeast this transcriptional control is dependent upon a different transcription factor called Loz1. In contrast to Zap1, which has a primary role in activating gene expression in low zinc, deletion of the *loz1* gene leads to the constitutive expression of *zrt1* and a regulatory *adh1* antisense transcript (*adh1*AS), suggesting that the primary function of Loz1 is to repress gene expression when zinc is in excess (Corkins *et al.*, 2013). Studies with Loz1 have also revealed different genes and pathways that are regulated by zinc availability. One novel Loz1 target gene is *gcd1*, which encodes glucose dehydrogenase 1 (Corkins *et al.*, 2017). In fission yeast this enzyme is part of the gluconate shunt which is a secondary route for directing glucose into the pentose phosphate pathway (Tsai *et al.*, 1995, Corkins *et al.*, 2017). As the pentose phosphate pathway plays a primary role in the regeneration of NADPH and produces ribose-5 phosphate sugars which are precursors of many other metabolic intermediates, the regulation of *gcd1* by Loz1 suggests that increased levels of one or more of these intermediates may be important for growth or survival in low zinc conditions.

The goals of this study were to further our knowledge of zinc homeostasis by identifying additional genes that are regulated by Loz1 and to test whether Loz1 directly binds to its target gene promoters to repress gene expression. By using ChIP-seq we show that Loz1 binds in a zinc-dependent manner to the sequence CGN(A/C)GATCNTY when zinc is in excess, highlighting a mechanism by which Loz1 is able to specifically repress target gene expression in high zinc. We also find that in high zinc Loz1 represses the expression of 27 genes that encode proteins and ncRNAs required for zinc homeostasis, as well as carbohydrate metabolism, the transport of small molecules, and non-covalent protein folding.

Results

Loz1 binds to target genes promoters in high zinc

In our previous studies we found that Loz1 negatively auto-regulates its own expression which leads to very low levels of the active Loz1 repressor accumulating in high zinc conditions (Corkins *et al.*, 2013). When we attempted to perform ChIP analysis using a functional Loz1GFP fusion protein that was expressed from the *loz1* promoter, we were unable to immunoprecipitate Loz1GFP from cells grown in high zinc, potentially due to the low levels of Loz1GFP protein that accumulate under this condition. To overcome this limitation, we generated a new construct to express Loz1GFP from a weaker derivative of the *pgk1* promoter that contained a deletion within the canonical TATA box (*pgk1*$^{\Delta TATA}$). To compare the strength of the *pgk1*$^{\Delta TATA}$ promoter to the *loz1* promoter (*loz1*^{p}), strains expressing Loz1GFP from these promoters were grown overnight in a zinc-limited minimal medium (ZL-EMM) (Choi *et al.*, 2018) supplemented with 0 (-Zn) or 100 μM Zn (+Zn) and crude protein extracts prepped for immunoblot analysis. The immunoblot analysis revealed that the *pgk1*$^{\Delta TATA}$-driven Loz1GFP accumulated in both low and high zinc conditions (Fig. 1A). When compared to cells expressing Loz1GFP from the *loz1* promoter, expression from the *pgk1*$^{\Delta TATA}$ promoter resulted in ~ 2-fold and ~ 7-fold higher levels of Loz1GFP in low and high zinc conditions, respectively.

To test whether expression of *loz1GFP* from the *pgk1*$^{\Delta TATA}$ promoter would affect Loz1-mediated gene expression, we co-expressed the Loz1GFP alleles described above with a *zrt1-lacZ* reporter and assayed β-galactosidase activity over a range of zinc levels. In cells expressing *pgk1*$^{\Delta TATA}$-Loz1GFP, growth in 100 μM zinc resulted in an ~600-fold reduction in *zrt1-lacZ* reporter activity, indicating that the activity of this fusion protein was regulated by zinc (Fig. 1B). However, at 0 μM zinc *zrt1-lacZ* reporter activity was 3-fold lower than that observed in *loz1*Δ expressing *loz1*^{p}-Loz1GFP, suggesting that over-expression of Loz1 also leads to higher levels of gene repression. When the association of *pgk1*$^{\Delta TATA}$-Loz1GFP with the *zrt1* and *adh4* promoters was examined using ChIP analysis, there was a large enrichment of Loz1GFP at both of these promoters in high zinc conditions (Fig. 1C). A similar enrichment was not observed at a promoter of a control gene (*pci2*) that is not regulated by zinc (Dainty *et al.*, 2008, Ehrensberger *et al.*, 2013). Although over-expression of Loz1 from the *pgk1*$^{\Delta TATA}$ promoter leads to higher levels of gene repression, these preliminary ChIP analyses suggested that the *pgk1*$^{\Delta TATA}$-driven Loz1GFP could be used to examine zinc-dependent changes in Loz1 DNA binding activity.

To determine if the recruitment of Loz1 to other promoter regions was dependent upon zinc, *loz1*Δ cells expressing *pgk1*$^{\Delta TATA}$-Loz1GFP were grown in ZL-EMM supplemented with 0 or 100 μM zinc, and purified DNA associated with Loz1GFP further analyzed by ChIP-seq (see Experimental procedures). 136 peaks were above peak-ID thresholds in at least three independent repeats. 98 of these peaks were located upstream of protein-coding genes or non-coding RNAs (Fig. 2A), whereas the remaining 38 peaks were detected within the coding regions of tRNAs or other small RNAs. Of the 98 peaks that were located within promoter regions, 60 were detected during growth in high zinc, 34 were detected in both high and low zinc conditions, and 4 were detected in low zinc only (Table S1 and S2). The most abundant peaks were detected in the high zinc conditions and included peaks mapping to the promoter regions of the known Loz1 target genes *adh4*, *zrt1*, and the *adh1AS* transcript (Fig. 2B). We also determined which peaks displayed a differential binding pattern in response to cellular zinc status. For these analyses we defined differential binding as a Loz1 peak that displayed a 2-fold increase in one condition as compared to the other condition. 63 Loz1 binding peaks were identified that were enriched in cells grown in high zinc as compared to low zinc, including *adh4*, *zrt1*, and *adh1AS* (Fig. 2C and Table S3). Only a single Loz1-binding peak was identified that was enriched in low zinc as compared to high zinc. This peak mapped to the promoter region of *ght8*, which encodes a putative hexose transporter.

As the *pgk1*$^{\Delta TATA}$-driven Loz1GFP protein accumulates at higher levels inside of cells relative to the endogenous Loz1 protein, it was possible that some of the ChIP peaks identified were false positives arising from over-expression. For example, many of the Loz1-binding peaks were found in the promoters of highly expressed genes (e.g. *pgk1*), which are commonly found as false positives in ChIP-seq studies (Park *et al.*, 2013). To determine which of the genes identified by ChIP-seq were bona fide Loz1 targets, we used RNA-seq to identify transcripts that accumulated in wild-type and *loz1*Δ cells following growth overnight in high zinc. As Loz1 is required for transcriptional repression when zinc is in excess, we predicted that Loz1 target genes would be: 1) expressed at a higher level in zinc-replete *loz1*Δ cells when compared to wild-type cells; 2) would be identified as a target gene in the ChIP-seq analysis; and 3) would contain a binding site for Loz1 in their promoter.

In the RNA-seq analysis 126 unique mRNAs accumulated significantly by ≥ 2-fold in zinc-replete *loz1*Δ cells. Of these, 24 were also identified as ChIP-seq targets, suggesting that these were the genes that were repressed by Loz1 in high zinc under steady state conditions (Fig. 3A). In order to validate these results, a number of transcripts were also analyzed by RNA blot analysis. In all cases deletion of *loz1* led to higher levels of the transcript accumulating in zinc-replete cells, consistent with these genes being regulated by Loz1 (Fig. 3B and 3C). There were also notable differences in the transcript profiles, which could potentially reflect variation in the recruitment of Loz1 to each promoter, or combinatorial effects of other regulatory proteins. As one example, higher levels of *dak2* transcripts were detected in *loz1*Δ cells relative to zinc-limited wild-type cells, suggesting that deletion of *loz1* results in increased levels of *dak2* transcripts by an alternative mechanism. In a few cases, known Loz1 targets were identified as strong ChIP targets and their fold induction in the RNA-seq analysis did not reach statistical significance (*adh1AS*), or they were identified as strong RNA-seq targets and their ChIP-seq peaks fell just below the threshold peak ID

(*loz1* and *SPBC1348.06c*). As the expression of these genes has previously been shown to be dependent upon Loz1 (Corkins *et al.*, 2013), they were also included as Loz1 target genes in further analyses.

To determine if the genes identified in the RNA-seq and/or ChIP-seq were under the control of any common regulatory elements, we next searched the promoter regions and ChIP-seq peaks for regulatory DNA motifs using the de novo computational motif discovery program Multiple Em for Motif Elicitation (MEME) (Bailey *et al.*, 2009). When the search was restricted to ChIP-seq peaks of genes repressed in high zinc in a Loz1-dependent manner, a consensus of CGN(A/C)GATCNTY was present in 16 peaks (Fig. 4A), the core of which resembled the GNNGATC sequence that was previously suggested to be important for Loz1-mediated gene repression (Corkins *et al.*, 2013). Related searches with other programs including HOMER, CONSENSUS, and Weeder revealed shorter motifs that also had a similar core CGNNGATC consensus (Fig. S1). No common consensus was identified when all ChIP-seq peaks were included in the analyses, or in ChIP-seq peaks that were not RNA-seq targets. From here on, the CGN(A/C)GATCNTY element was named the Loz1 Response Element (LRE).

The LRE is necessary for Loz1-mediated gene repression

To validate that the LRE was required for Loz1-mediated gene repression, we used site directed mutagenesis to introduce nucleotide substitutions in putative elements in a *SPBC1348.06c-lacZ* reporter. We used this reporter as *SPBC1348.06c* was a highly regulated gene in the RNA-seq analysis, and we had previously found that the activity of the *SPBC1348.06c-lacZ* reporter was tightly regulated by Loz1 and zinc (Corkins *et al.*, 2013). The MEME analysis indicated that the *SPBC1348.06c* promoter contained a single LRE (5'-CGACGATCATG-3') at nucleotide positions −147 to −137 relative to the translational ATG (Fig. 4B). In addition to this element, we identified two closely related sequences at positions −380 to −370 (5'-GGAAGATCTAC-3') and −130 to −140 on the reverse strand (5'-CGTAGATCATG-3'). To assess whether these elements were required for Loz1-mediated gene repression, we generated constructs containing nucleotide substitutions that targeted the highly conserved 'G' (at position 5) and 'A' (at position 6) in LRE2 and LRE3, and the highly conserved 'T' (at position 7) and 'C' (at position 8) in LRE1 (Fig. 4B). Consistent with previous studies we found that the activity of the *SPBC1348.06c-lacZ* reporter was ~50-fold lower in zinc-replete cells, in a manner that was dependent upon Loz1 (Fig. 4C strains 1 and 9). Nucleotide substitutions that targeted individual LREs reduced Loz1-mediated repression by ~10–20%, with substitutions targeting LRE2 having the most significant effect (Fig. 4C strains 3–5). When the mutations disrupting LRE1 and LRE2 were combined, there was no further reduction (Fig. 4C strain 6). However, when nucleotide substitutions were introduced that targeted all three LREs, Loz1-mediated gene repression was eliminated (Fig. 4C strain 7). Loz1-mediated gene repression was also eliminated when nucleotide substitutions were introduced that targeting the G and A in all three LREs (data not shown). The results are consistent with at least one LRE being required for Loz1-mediated gene repression.

To gain additional evidence that LREs were required for Loz1 regulation we tested whether this element was required for the Loz1-mediated repression of a *gcd1-lacZ* reporter. The *gcd1* promoter contains two putative LREs at positions −303 to −293 and −384 to −374, relative to the transcriptional start site (Fig. 5A). To assess the role of the individual elements we generated long and short *gcd1-lacZ* reporter constructs containing one or both of the elements. Growth in high zinc led to a 12-fold reduction in reporter activity of the longer *gcd1-lacZ* reporter, in a manner that was dependent upon Loz1 (Fig. 5B strains 2 and 7). The shorter reporter was also regulated by zinc and Loz1. However, this reporter had higher levels of activity in low zinc, and growth in high zinc only resulted in an ~2-fold decrease in β-galactosidase activity (Fig. 5B, strain 3). To test whether LRE1 was required for the 2-fold decrease in the activity of the shorter reporter we substituted the highly conserved 'C' at position 8 in the LRE to a 'G'. While this mutation was expected to interfere with Loz1-mediated gene repression, it did not significantly alter the level of gene repression observed in high zinc conditions (Fig. 5B strain 4).

Potential explanations of the above results are that Loz1 binds to additional sites in the *gcd1* promoter, or that Loz1 regulates the expression of other proteins or RNAs that affect *gcd1* expression. To further probe Loz1 DNA binding specificity, we used electrophoretic mobility shift analysis (EMSA) to screen for nucleotide substitutions that affected Loz1 DNA binding in vitro. The recombinant Loz1 protein used for these analyses consisted of the C-terminal amino acid residues 426–522 containing two C_2H_2-type zinc fingers and an adjacent accessory domain. A DNA-protein complex was detected when purified $Loz1^{426-522}$ was incubated with ^{32}P-labeled double-stranded oligomers containing the 'wild-type' motif 5'-CGNMGATCNTY-3 (Fig. S2). The formation of this complex was also inhibited by incubation with competitor unlabeled 'wild-type' oligomers indicating that Loz1 binds to this sequence in a site-specific manner. When EMSAs were performed using related oligomers containing systematic nucleotide substitutions to the core LRE sequence, no DNA-protein complexes were detected when nucleotide substitutions were introduced that altered the 'G' at position 2, and the 'A', 'T', or 'C', at positions 5 to 7 (Fig. S3 and S4). Substitutions of the G at position 5 with a C and T also led to the loss of complex formation, whereas substitutions altering nucleotides at positions 3 or 4 in the LRE had no effect on DNA-complex formation (Fig. S3 and S4).

The above screen suggested that the G at position 2 in the LRE and the core ATC nucleotides at positions 6–8 were critical for site-specific Loz1 DNA binding activity. They also suggested that a G or A can be present at position 5. When we searched the shorter *gcd1* promoter region for motifs with a core sequence of 5'-NGNN(G/A)ATCNNN-3', we found one additional motif on the reverse strand at position −276 to −286 (5'-TGCAAATCTTC-3'), which we designated *gcd1* LRE3 (Fig. 5A LRE3). When mutations were introduced targeting key nucleotides in *gcd1* LRE3, mutation of this element led to a reduction in Loz1-mediated gene repression in high zinc, whereas disruption of both LRE2 and LRE3 led to a further loss of Loz1-mediated gene expression (Fig. 5B strains 5 and 6). These results are consistent with Loz1 binding to derivatives of the LREs with an A at position 5. They also suggest that Loz1-mediated gene repression is relatively complex, and that multiple factors including the LRE sequence, the total number of LREs within a

promoter, and the position of the LREs, may affect the levels of gene repression observed in high zinc conditions.

The LRE is sufficient for Loz1-mediated gene repression

To determine if the LRE was sufficient for Loz1-dependent gene repression, we developed constructs to express a minimal *CYC1-lacZ* (^{Min}*CYC1-lacZ*) reporter in *S. pombe* (Fig. 6A). This reporter contains the well characterized minimal region of the *CYC1* promoter from *S. cerevisiae*, which includes the canonical TATA box, but not any UASs (Bachhawat *et al.*, 1995, Zhao *et al.*, 1998). As this minimal system could potentially contain binding sites for transcription factors from *S. pombe*, we first integrated the ^{Min}*CYC1-lacZ* reporter into the *leu1* locus of wild-type and *loz1*Δ cells and measured β-Galactosidase activity following growth in low and high zinc. As shown in Fig. 6B, very low levels of β-Galactosidase activity were observed in cells expressing the ^{Min}*CYC1-lacZ* reporter, suggesting that this minimal promoter region does not contain sequences that function as UASs in *S. pombe*.

We next introduced a thiamine-regulatory sequence (TRS) 241 bp upstream of the translational ATG (Fig. 6A). The TRS is a previously mapped cis-acting element that is required for strong activation of the *nmt1* promoter (Zurlinden & Schweingruber, 1997). Consistent with this sequence containing a binding site for a transcriptional activator, the insertion of the TRS led to an ~600-fold increase in β-Galactosidase activity (Fig. 6B). This increase in activity was also independent of Loz1 and was not affected by cellular zinc status. When an LRE was inserted into a similar site, it was not able to confer any increase in activity.

To test whether the LRE was sufficient for Loz1-mediated gene repression, we inserted 1 or 2 copies of the overlapping LRE1 and LRE2 from the *SPBC1348.06c* promoter, upstream of the TRS (Fig. 6C). We introduced multiple copies of the LRE for these studies because it is unclear how Loz1 facilitates gene repression, and whether other factors such as distance of the LRE from UAS's and other promoter elements are important for Loz1-mediated repression. In this minimal system, the insertion of two LREs upstream of the TRS resulted in ~1.5-fold decrease in β-galactosidase activity in zinc-replete cells, whereas the introduction of 4 LREs led to a ~5-fold decrease (Fig. 6D). In both cases the zinc-dependent decrease in β-galactosidase activity was dependent upon Loz1. These results are consistent with the LRE being sufficient for Loz1-mediated gene repression.

As the LRE sequence was required and sufficient for Loz1-mediated gene repression we searched the promoters of the putative Loz1 target genes for consensus and non-consensus LREs. 25 of the 27 target genes contained at least one NGNNGATCNNN motif within the ChIP-seq. peak or within 100 bp of the peak (Table 1). Although two ChIP-seq peaks did not contain this motif, multiple NGNNAATCNNN sequences were present suggesting that Loz1 may bind to non-consensus elements at these promoters. As these genes are Loz1 ChIP-seq targets and are repressed in high zinc in a manner that is dependent upon Loz1, we propose that these 27 genes form the Loz1 regulon in fission yeast. As discussed below, these genes encode proteins that have known roles in zinc homeostasis, small molecule transport, covalent protein folding, and carbohydrate metabolism.

Discussion

In this study we examined the role of the Loz1 transcription factor in controlling gene expression in response to cellular zinc status. We have found that at the majority of promoters Loz1 binds to LREs in high zinc conditions and that the recruitment of Loz1 to these elements is associated with lower levels of gene expression. Based on these observations we propose that the primary function of Loz1 is gene repression when zinc is in excess.

When expressed from the constitutive *pgk1*$^{\Delta TATA}$ promoter, ~ 75% of the genes identified as Loz1 target genes had a Loz1-binding peak that was enriched in high zinc growth conditions (Table 1 and S3). As Loz1 is localized to the nucleus under all growth conditions (Corkins *et al.*, 2013), these results are consistent with Loz1 DNA binding activity being regulated by zinc. How might zinc affect Loz1 DNA binding function? Functional dissection of the Loz1 protein has shown that the smallest region that is able to confer zinc-dependent gene repression maps to its last 96 amino acids (Ehrensberger *et al.*, 2014). This same small region contains two C_2H_2 zinc finger domains and an adjacent accessory domain, both of which are necessary for Loz1 DNA binding activity in vitro and Loz1-mediated gene repression in vivo (Ehrensberger *et al.*, 2014). As the minimal zinc responsive domain of Loz1 contains two C_2H_2 zinc finger domains, one potential explanation for the zinc-responsiveness of the Loz1 protein is that one or both of these domains bind zinc with a low affinity. In this model the low affinity zinc finger domain(s) would be in a largely unstructured apo-form in low zinc conditions preventing Loz1 from binding to DNA. On the other hand, when there were adequate levels of intracellular zinc, the zinc finger domain(s) would bind zinc and fold into a conformer that permits DNA binding and gene repression.

Our current results also do not exclude models where both of the zinc finger domains are occupied with zinc under all growth conditions, and therefore an alternative regulatory event controls Loz1 DNA binding activity. For example, in some transcription factors post-translational modifications of key residues in zinc finger domains or their linker regions can interfere with DNA binding (Dovat *et al.*, 2002, Kluska *et al.*, 2018). Other viable models therefore include the possibility that Loz1 is post-translationally modified or interacts with other regulatory factors in a manner that is dependent upon cellular zinc status, and that this regulatory event affects DNA binding function. Studies of other eukaryotic zinc-responsive transcription factors including MTF-1 and Zap1 have shown that they are able to sense changes in intracellular zinc levels using regulatory zinc finger domains (Bird *et al.*, 2003, Chen *et al.*, 1999, Gunther *et al.*, 2012, Wang *et al.*, 2006). We therefore favor a model where Loz1 is the direct sensor of zinc in yeast. Our ongoing experiments are currently testing whether one or both of the Loz1 zinc finger domains bind zinc with a reduced affinity.

By examining the activity of the *pgk1*$^{\Delta TATA}$-driven Loz1GFP we found that the over-expression of Loz1GFP results in higher levels of gene repression under low zinc conditions. If Loz1 DNA binding activity is dependent upon zinc, why would overexpression of Loz1 in a zinc-limited cell lead to increased gene repression? One possible explanation is that the levels of Loz1 within cells are not sufficient to occupy all of the Loz1 binding sites within

the genome. In this scenario, an increase in the total levels of Loz1 could result in a higher number of active Loz1 proteins under a given condition, which in turn may lead to an increased occupancy of LREs and a higher level of gene repression. An alternative possibility is that a yet to be identified factor(s) maintains Loz1 in its inactive state in low zinc. While we have not yet identified any additional factors required for Loz1-mediated gene repression, there are precedents for this type of regulation. For example, in *S. cerevisiae* the inactivation of the transcription factor Hap1 in low heme is dependent upon the recruitment of Ssa-type Hsp70 molecular chaperones that mask the Hap1 DNA binding and transactivation domains (Hon *et al.*, 2001). These interactions are critical to maintain Hap1 in an inactive state as reduced expression of Hsp70 chaperones or overexpression of Hap1 both lead to the derepression of Hap1 target genes. In fission yeast a related model could exist where additional proteins maintain Loz1 in its inactive state in low zinc, and over-expression of Loz1 overrides this mechanism.

While the preferentially recruitment of Loz1 to its target gene promoters in high zinc provides a simple explanation of how gene repression occurs in a manner that is dependent upon zinc, approximately 25% of the genes that were identified as Loz1 targets had a Loz1-binding peak that was enriched in high and low zinc conditions (Fig. 2C and Table S3). Given that the Loz1GFP fusion protein used for the ChIP-seq analysis was over-expressed, we currently cannot eliminate the possibility that the ability of Loz1 to bind to these promoters in a zinc-independent manner is an artefact of the higher levels of Loz1 in these cells. However, studies of different zinc-responsive transcription factors have found that these proteins often contain multiple zinc-responsive domains that are independently regulated by zinc (Frey & Eide, 2011, Wilson & Bird, 2016, Gunther *et al.*, 2012). It is therefore possible that Loz1-mediated gene repression at some promoters may be more complex, with Loz1 being bound under all conditions and an alternative regulatory mechanism triggering its inactivation in high zinc.

By analyzing ChIP-seq and RNA-Seq targets we identified 27 genes that are repressed in high zinc in a Loz1-dependent manner. Of these genes, eight have homologs or functional homologs in *S. cerevisiae* that are regulated by Zap1 (*zrt1*, *adh4*, *adh1AS*, *tpx1*, *pof1*, *SPAC977.05c*, *SPBC1348.06c, SPBPB2B2.15*). Given the considerable evolutionary distance between budding and fission yeast, the conserved regulation of these genes in both systems suggests that this subset of genes have particularly important roles in zinc homeostasis or for survival when zinc levels are low. Consistent with this hypothesis, Zrt1 is critical for the survival of *S. pombe* and *S. cerevisiae* under zinc-deficient conditions (Zhao & Eide, 1996, Boch *et al.*, 2008). The *ADH4* and *TSA1* genes are also required for growth in low zinc in *S. cerevisiae* (North *et al.*, 2012).

The identification of *tpx1* (*TSA1* in *S. cerevisiae*) and *pof1* (*MET30* in *S. cerevisiae*) as Loz1 target genes highlight two new conserved zinc-regulated pathways. In *S. cerevisiae* the peroxiredoxin Tsa1 is critical for survival in low zinc because it has a molecular holdase function which prevents aggregation of unfolded and misfolded proteins (MacDiarmid *et al.*, 2013, Wu *et al.*, 2007). While it is not yet known if the molecular chaperone function of Tpx1 is critical for survival of fission yeast in low zinc, the conserved regulation of peroxiredoxin gene expression by zinc suggests that increased levels of unfolded and

misfolded proteins may be a widespread problem in low zinc conditions. Based on studies of Met30 in *S. cerevisiae* the regulation of *pof1* by Loz1 could be a mechanism to help reduce oxidative stress under conditions of zinc deficiency. In *S. cerevisiae*, Met30 facilitates the degradation of Met4, a transcription factor required for the expression of sulfate assimilation genes (Wu *et al.*, 2009). Since sulfate assimilation requires high levels of NADPH, an important cofactor for oxidative stress defense, the net result of increased expression of *MET30* in low zinc is reduced sulfate assimilation and conservation of NADPH. In fission yeast Pof1 controls the degradation of Zip1, a transcription factor required for the expression of sulfate assimilation genes (Harrison *et al.*, 2005, Guo *et al.*, 2012). The Loz1-dependent regulation of *pof1* expression could therefore be a related mechanism to conserve NADPH. It is also noteworthy that *gcd1* is a Loz1 target and that derepression of *gcd1* expression in low zinc results in glucose being directed into the pentose phosphate pathway via the gluconate shunt (Corkins *et al.*, 2017). As the pentose phosphate pathway is a major route for the regeneration of NADPH, *S. pombe* may rely on multiple mechanisms to combat higher levels of oxidative stress in low zinc.

In addition to identifying conserved regulatory pathways Loz1 controls the expression of many unique genes. As examples, Loz1 target genes include *puf5*, which encodes a member of the pumilio family of RNA binding proteins, and *pyp2* which encodes a putative tyrosine phosphatase. As 102 additional transcripts were expressed at higher levels in *loz1*Δ cells that were not Loz1 ChIP-seq targets, it is tempting to speculate that alterations in the expression of these Loz1 target genes may affect the expression of other genes by influencing mRNA decay or by affecting the activity of other transcription factors. Another new Loz1 target gene is *dak2*, which encodes dihydroxyacetone kinase, an enzyme that is involved in the breakdown of glycerol via a dihydroxyacetone phosphate (DHAP) intermediate. In the DHAP pathway glycerol is oxidized to dihydroxyacetone, which is then phosphorylated to DHAP by Dak1 or Dak2 (Matsuzawa *et al.*, 2010). Why would *dak2* expression be regulated by Loz1? One potential explanation is that in low zinc there is a significant reduction in levels of the zinc-requiring enzyme aldolase, which catalyzes the reversible cleavage of fructose 1,6, bisphosphate into DHAP and Glyceraldehyde-3-phosphate (G3P) (Wang *et al.*, 2018). As increased Dak2 activity would increase the generation of DHAP, increased expression of *dak2* in low zinc could be a mechanism to compensate for reduced aldolase activity under this condition. While additional experiments are needed to test this hypothesis, they highlight that studies with other Loz1 target genes will likely provide additional insight into the molecular consequences of zinc deficiency.

Experimental Procedures

Strains and growth conditions

The yeast strains used in this study are shown in Table S4. All strains were grown in YES medium supplemented with 3% glucose and 225 mg/l leucine, 225 mg/l uracil and 338 mg/l adenine, or in Zinc-Limited Edinburgh Minimal Medium (ZL-EMM) which is a derivative of EMM which does not contain zinc (Choi *et al.*, 2018). Prior to inoculation in ZL-EMM, cells were pre-grown to exponential phase in Yeast Extract with supplements (YES) medium and washed twice with ZL-EMM with no added zinc.

Plasmid construction

To generate pgk1$^{\Delta TATA}$-Loz1GFP a cloning strategy was used that first involved generating Pgk1-Loz1-GFP, which contains a fusion of the *loz1* and GFP open reading frames under the control of 840 bp of the *pgk1* promoter and its 5'UTR. To create Pgk1-Loz1-GFP, the *pgk1* promoter and 5'UTR were amplified by PCR using primers containing Kpn1/EcoRI sites. The Kpn1/EcoRI digested PCR product was then inserted into similar sites of the vector JK-GFP (Corkins *et al.*, 2013) to generate JK-pgk1-GFP. To generate an in-frame fusion of Loz1 to GFP, the *loz1* open reading frame without its stop codon was released from the vector pSK-*loz1* (Corkins *et al.*, 2013) by digestion with EcoRI and BamHI and subcloned into similar sites in the vector JK-pgk1-GFP to generate *pgk1*-Loz1GFP. To generate *pgk1*$^{\Delta TATA}$-Loz1GFP, QuikChange mutagenesis (Agilent) was used to delete the first four nucleotides of the canonical TATA box found at position −85 to −82 in the *pgk1* promoter relative to the translational ATG. The construction of the *zrt1-lacZ* reporter was described previously (Ehrensberger *et al.*, 2014). To create the *SPBC1348.06c*-lacZ reporter a DNA fragment encompassing positions +3 to −1205 bp of the *SPBC1348.06c* promoter and ORF was amplified using PCR. This fragment was inserted into the EagI and BamHI sites of the vector JK-lacZ (Ehrensberger *et al.*, 2013). Primers for these reactions were designed so that the translational ATG of *SPBC1348.06c* was inserted in frame with the *lacZ* coding region. Derivatives of this vector containing nucleotide substitutions within LREs were generated by cloning overlapping PCR products containing the following nucleotide substitutions shown in bold: LRE1 (5'-CGTAGA**GG**ATG-3'); LRE2 (5'-CGAC**CC**TCATA-3'); and LRE3 (5'-GGAA**CC**TCTAC-3'). Constructs containing substitutions in multiple LREs, were generated using the vector templates that already contained substitutions in alternative LREs. The construction of the reporter *gcd1-lacZ*, which contains 1452 bp of the *gcd1* promoter and 5'UTR was described previously (Corkins *et al.*, 2017). The shorter *gcd1* reporter was generated in a similar manner and contains 1108 bp of the *gcd1* promoter and 5'UTR fused to the *lacZ* open reading frame. The minimal *CYC1* promoter was generated by using PCR to amplify a 700 bp minimal *CYC1* promoter fragment from the vector pNB404 (Bachhawat *et al.*, 1995). Primers were designed to introduce this fragment into the SacII/BamHI sites of the vector JK-lacZ. Cloning of oligonucleotide TRS insert was performed as described by (Zhao *et al.*, 1998). Briefly, complementary oligonucleotides containing suitable overhangs to clone into the SalI restriction sites were phosphorylated using T4 polynucleotide kinase, annealed in the presence of 0.32 × SSC, and were subcloned into SalI digested JK-lacZ. Combinations of LREs from the *SPBC1348.06c* promoter were introduced upstream of the TRS by two-step overlapping PCR (Ho *et al.*, 1989). All PCR products generated by overlapping PCR were inserted into the SacII/BamHI of JK-lacZ. All constructs were confirmed by sequencing.

ChIP Analysis

For ChIP analysis 75 ml of the strain *loz1*Δ *pgk1*$^{\Delta TATA}$-Loz1GFP were grown to an OD^{600} of ~6.0 in ZL-EMM supplemented with or without 100 μM Zn^{2+} and were treated with 1% formaldehyde for 10 min at room temperature. Crosslinking was quenched by the addition of 250 mM glycine. Cells were then washed, resuspended in the lysis buffer (50mM Hepes-KOH pH 7.5, 140mM NaCl, 1mM EDTA, 1% (v/v) Triton X-100, 0.1% (w/v) sodium

deoxycholate, 0.4mM DTT, and protease inhibitors) and lysed by vortexing for 7 × 1 min in the presence of zirconium beads. To obtain cross-linked chromatin, cell lysates were centrifuged at 14,000 rpm for 5 min and the supernatant discarded. After centrifugation, cross-linked chromatin was resuspended in lysis buffer, DNA sheared to an average length of 500 bp by sonication, and cell debris removed by centrifugation at 14000 rpm for 5 min. For immunoprecipitations, chromatin solutions were incubated with anti-GFP antibodies (Abcam Ab290) and protein A magnetic beads (Invitrogen™ Dynabeads™ Protein A) overnight at 4°C. After Immuno-complexes were harvested the crosslinks were reversed by heating at 65°C for 5–7 hrs and DNA purified by Qiagen PCR purification kit. The percent input method was used to calculate the signal of enrichment as described by (Chung *et al.*, 2014).

ChIP-seq Analysis

ChIP seq samples were prepared as described above with the exception that the sonication step was performed using a Covaris Evolution ultrasonicator. The ChIP-seq Methodology performed by the Institute for Genomic Medicine at Nationwide Children's Hospital. ChIP-seq libraries were constructed from 5 ng of fragmented ChIP DNA using NEB Ultra II FS library prep kit (New England Biolabs, Ipswhich MA). Briefly, DNA fragment ends were 5´ Phosphorylated, dA-tailed, and ligated with a unique, dual UMI indexed adaptor (Integrated DNA Technologies, Iowa). Following purification, using a magnetic-bead based approach (AMPure XP System), adaptor-ligated DNA was amplified by 8–9 PCR cycles. Quality of libraries were determined via Agilent 2200 TapeStation using High Sensitivity D1000 reagents, and quantified using Kappa SYBR®Fast qPCR kit (KAPA Biosystems, Inc, MA). Approximately, 4 million paired-end 150 bp sequence reads were generated per sample using Illumina MiniSeq platform. Sequencing reads were analyzed using the HOMER suite (Heinz *et al.*, 2010). Tag directories were created using HOMER makeTagDirectory with -fragLength parameter manually specified for each sample. The makeUCSCfile program was used to generate bed graph files used for visualization in the Integrative Genomics Viewer (Robinson *et al.*, 2011). The findPeaks program with the -style option set to 'factor' was used for peak-calling and findMotifsGenome.pl was used to identify motifs enriched in the ChIP-seq peaks. Differentially binding analysis for ChIP-seq signals between low and high zinc replicates was conducted using the Diffbind package, which uses the TMM normalization method from the edgeR package to identify differential peaks (Afgan *et al.*, 2016, Ross-Innes *et al.*, 2012, Stark & Brown, 2011).

Motif discovery and Enrichment in Loz1-regulated genes

For analysis of conserved promoter elements, the MEME motif finder was accessed at meme-suite.org and run using default parameters (Bailey *et al.*, 2009). Weeder and CONSENSUS were run at default parameter settings using their respective standalone applications for Linux (Pavesi *et al.*, 2004, Hertz & Stormo, 1999).

Protein extraction and Immunoblot analysis

Crude protein extracts were prepared using a Trichloroacetic Acid (TCA) precipitation as described by (Peter *et al.*, 1993). Briefly 5 ml of cells were harvested by centrifugation for 2 min at 3500 rpm. Cell pellets were resuspended in 0.5 ml of ice-cold buffer A (20 mM Tris

(pH 8.0), 50 mM NH_4OAc, 0.5 mM EDTA, 0.2 mM phenylmethylsulfonyl fluoride) and were immediately mixed with 0.5 ml of ice cold 20% trichloroacetic Acid. Cells were then vortexed in the presence of glass beads for 2 × 0.5 min, with 2 min cooling on ice in-between. The supernatant was the placed into a new tube, proteins pelleted by centrifugation for 10 min at 12,000 rpm, and the pellet resuspended in trichloroacetic acid-sample buffer (3% SDS, 100 mM Tris base pH 11, 3 mM DTT). Extracts were then boiled for 10 min and insoluble cell debris pelleted by centrifugation for 2 min at 12,000 rpm. Proteins were separated by SDS-PAGE polyacrylamide gene electrophoresis followed by immunoblotting to a nitrocellulose membrane. Immunoblots were probed with anti-GFP (G1544, Sigma) and anti-Act1 (ab3280–500) primary antibodies and IRDye800CW-conjugated anti-mouse IgG (LI-COR) and IRDye680-conjugated anti-rabbit IgG (LI-COR) secondary antibodies. An Odyssey infrared image system (LI-COR) was used for visualization and analysis of signal intensities.

β-galactosidase assays

β-galactosidase assays were performed as described by (Guarente, 1983). Briefly in these assays 1 ml of cells are resuspended in lacZ buffer (0.06 M $Na_2HPO_4.7H_2O$, 0.04M $NaH_2PO_4.H_2O$, 0.01 M KCl, and 0.001 M $MgSO_4$) and lysed by vortexing for 10 s in the presence of 0.05 ml of $CHCl_3$ and 0.05 ml of 0.1% SDS. β-galactosidase activity was determined by monitoring the hydrolysis of the substrate *o*-Nitrophenyl-β-D-galactosidase (ONPG), and was calculated using the following equation: (ΔA 420 × 1000)/(min × ml of culture × culture absorbance at 600 nm). Error bars represent the standard deviation of values obtained from 3 independent repeats.

RNA-blot hybridizations and RNA-seq analysis

For RNA blot analyses total RNA was purified from the indicated cells using the hot acidic phenol method (Collart & Oliviero, 1993). Depending on transcript abundance, between 5–20 μg of denatured total RNA was separated on formaldehyde gels and transferred to nylon membrane according to the method described by Sambrook et al., (Sambrook & Russell, 2001). Following transfer RNA blots were incubated with single stranded ^{32}P-labeled RNA probes that were generated from purified PCR products using the Ambion™ MAXIscript™ T7 In Vitro Transcription kit according to manufacturer's instructions. Signal intensities representing transcript abundance were visualized using GE Typhoon FLA 9500. For RNA seq analysis wild-type and *loz1* deletion strains were grown to mid log phase in zinc-limited EMM supplemented with 100 μM Zn. Total RNA was isolated using the RiboPureTM RNA Purification Kit for yeast (ThermoFisher Scientific) according to the manufacturer's instructions and subsequent library preparation and next generation sequencing performed by Beckman Coulter Genomics. Reads were aligned to the *S. pombe* reference genome using Hisat2 (Kim *et al.*, 2015), and transcripts assembled and FPKM (fragments per kb for a million reads) values determined using Cufflinks (Trapnell *et al.*, 2012). Following normalization, differential expression of transcripts was assessed with cuffdiff of the cufflinks suite, and significant genes identified based on a false discovery rate of 0.05 (Trapnell *et al.*, 2012, Trapnell *et al.*, 2013).

Data availability

The RNA-Seq and ChIP-Seq data generated in this study were submitted to the Gene Expression Omnibus 347. The accession number for both data sets (SuperSeries record) is GSE130846. https://www.ncbi.nlm.nih.gov/geo/query/acc.cgi?acc=GSE130846

Supplementary Material

Refer to Web version on PubMed Central for supplementary material.

Acknowledgements

We gratefully acknowledge the IGM Genomic Services Laboratory at Nationwide Children's hospital for assistance with ChIP-seq analysis, and thank members of Bird and Foster labs and Dr. R. Michael Townsend for critical reading of the manuscript. This work was supported by NIH grant GM105695 Sciences grant, and by the Office of the Director, National Institutes of Health of the National Institutes of Health under Award Number S10OD023582.

References

Afgan E, Baker D, van den Beek M, Blankenberg D, Bouvier D, Cech M, et al., (2016) The Galaxy platform for accessible, reproducible and collaborative biomedical analyses: 2016 update. Nucleic Acids Res 44: W3–W10. [PubMed: 27137889]

Andreini C, Bertini I, and Rosato A (2009) Metalloproteomes: a bioinformatic approach. Acc Chem Res 42: 1471–1479. [PubMed: 19697929]

Anzilotti C, Swan DJ, Boisson B, Deobagkar-Lele M, Oliveira C, Chabosseau P, et al. (2019) An essential role for the Zn(2+) transporter ZIP7 in B cell development. Nat Immunol 20: 350–361. [PubMed: 30718914]

Bachhawat N, Ouyang Q, and Henry SA (1995) Functional characterization of an inositol-sensitive upstream activation sequence in yeast. A cis-regulatory element responsible for inositol-choline mediated regulation of phospholipid biosynthesis. J Biol Chem 270: 25087–25095. [PubMed: 7559640]

Bailey TL, Boden M, Buske FA, Frith M, Grant CE, Clementi L, et al. (2009) MEME SUITE: tools for motif discovery and searching. Nucleic Acids Res 37: W202–208. [PubMed: 19458158]

Bird AJ (2015) Cellular sensing and transport of metal ions: implications in micronutrient homeostasis. J Nutr Biochem 26: 1103–1115. [PubMed: 26342943]

Bird AJ, Gordon M, Eide DJ, and Winge DR (2006) Repression of ADH1 and ADH3 during zinc deficiency by Zap1-induced intergenic RNA transcripts. EMBO J 25: 5726–5734. [PubMed: 17139254]

Bird AJ, McCall K, Kramer M, Blankman E, Winge DR, and Eide DJ (2003) Zinc fingers can act as Zn2+ sensors to regulate transcriptional activation domain function. EMBO J 22: 5137–5146. [PubMed: 14517251]

Boch A, Trampczynska A, Simm C, Taudte N, Kramer U, and Clemens S (2008) Loss of Zhf and the tightly regulated zinc-uptake system SpZrt1 in Schizosaccharomyces pombe reveals the delicacy of cellular zinc balance. FEMS Yeast Res 8: 883–896. [PubMed: 18637840]

Chen X, Chu M, and Giedroc DP (1999) MRE-Binding transcription factor-1: weak zinc-binding finger domains 5 and 6 modulate the structure, affinity, and specificity of the metal-response element complex. Biochemistry 38: 12915–12925. [PubMed: 10504263]

Choi S, Hu YM, Corkins ME, Palmer AE, and Bird AJ (2018) Zinc transporters belonging to the Cation Diffusion Facilitator (CDF) family have complementary roles in transporting zinc out of the cytosol. PLoS Genet 14: e1007262. [PubMed: 29529046]

Chowanadisai W, Lonnerdal B, and Kelleher SL (2006) Identification of a mutation in SLC30A2 (ZnT-2) in women with low milk zinc concentration that results in transient neonatal zinc deficiency. J Biol Chem 281: 39699–39707. [PubMed: 17065149]

Chung D, Barker BM, Carey CC, Merriman B, Werner ER, Lechner BE, et al. (2014) ChIP-seq and in vivo transcriptome analyses of the Aspergillus fumigatus SREBP SrbA reveals a new regulator of the fungal hypoxia response and virulence. PLoS Pathog 10: e1004487. [PubMed: 25375670]

Coleman JE (1992) Zinc proteins: enzymes, storage proteins, transcription factors, and replication proteins. Annu Rev Biochem 61: 897–946. [PubMed: 1497326]

Collart M, and Oliviero S (1993) Preparation of Yeast RNA. Current Protocols in Molecular Biology 23: 13.12.11–13.12.15.

Corkins ME, May M, Ehrensberger KM, Hu YM, Liu YH, Bloor SD, et al. (2013) Zinc finger protein Loz1 is required for zinc-responsive regulation of gene expression in fission yeast. Proc Natl Acad Sci U S A 110: 15371–15376. [PubMed: 24003116]

Corkins ME, Wilson S, Cocuron JC, Alonso AP, and Bird AJ (2017) The gluconate shunt is an alternative route for directing glucose into the pentose phosphate pathway in fission yeast. J Biol Chem 292: 13823–13832. [PubMed: 28667014]

Dainty SJ, Kennedy CA, Watt S, Bahler J, and Whitehall SK (2008) Response of Schizosaccharomyces pombe to zinc deficiency. Eukaryot Cell 7: 454–464. [PubMed: 18203864]

Dovat S, Ronni T, Russell D, Ferrini R, Cobb BS, and Smale ST (2002) A common mechanism for mitotic inactivation of C2H2 zinc finger DNA-binding domains. Genes Dev 16: 2985–2990. [PubMed: 12464629]

Ehrensberger KM, Corkins ME, Choi S, and Bird AJ (2014) The double zinc finger domain and adjacent accessory domain from the transcription factor loss of zinc sensing 1 (loz1) are necessary for DNA binding and zinc sensing. J Biol Chem 289: 18087–18096. [PubMed: 24831008]

Ehrensberger KM, Mason C, Corkins ME, Anderson C, Dutrow N, Cairns BR, et al. (2013) Zinc-dependent regulation of the Adh1 antisense transcript in fission yeast. J Biol Chem 288: 759–769. [PubMed: 23223230]

Eide DJ (2009) Homeostatic and adaptive responses to zinc deficiency in Saccharomyces cerevisiae. J Biol Chem 284: 18565–18569. [PubMed: 19363031]

Frey AG, and Eide DJ (2011) Roles of two activation domains in Zap1 in the response to zinc deficiency in Saccharomyces cerevisiae. J Biol Chem 286: 6844–6854. [PubMed: 21177862]

Guarente L (1983) Yeast promoters and lacZ fusions designed to study expression of cloned genes in yeast. Methods Enzymol 101: 181–191. [PubMed: 6310321]

Gunther V, Lindert U, and Schaffner W (2012) The taste of heavy metals: gene regulation by MTF-1. Biochim Biophys Acta 1823: 1416–1425. [PubMed: 22289350]

Guo L, Ghassemian M, Komives EA, and Russell P (2012) Cadmium-induced proteome remodeling regulated by Spc1/Sty1 and Zip1 in fission yeast. Toxicol Sci 129: 200–212. [PubMed: 22610605]

Harrison C, Katayama S, Dhut S, Chen D, Jones N, Bahler J, and Toda T (2005) SCF(Pof1)-ubiquitin and its target Zip1 transcription factor mediate cadmium response in fission yeast. EMBO J 24: 599–610. [PubMed: 15660136]

Heinz S, Benner C, Spann N, Bertolino E, Lin YC, Laslo P, et al. (2010) Simple combinations of lineage-determining transcription factors prime cis-regulatory elements required for macrophage and B cell identities. Mol Cell 38: 576–589. [PubMed: 20513432]

Hertz GZ, and Stormo GD (1999) Identifying DNA and protein patterns with statistically significant alignments of multiple sequences. Bioinformatics 15: 563–577. [PubMed: 10487864]

Ho SN, Hunt HD, Horton RM, Pullen JK, and Pease LR (1989) Site-directed mutagenesis by overlap extension using the polymerase chain reaction. Gene 77: 51–59. [PubMed: 2744487]

Hon T, Lee HC, Hach A, Johnson JL, Craig EA, Erdjument-Bromage H, et al. (2001) The Hsp70-Ydj1 molecular chaperone represses the activity of the heme activator protein Hap1 in the absence of heme. Mol Cell Biol 21: 7923–7932. [PubMed: 11689685]

Jeong J, Walker JM, Wang F, Park JG, Palmer AE, Giunta C, et al. (2012) Promotion of vesicular zinc efflux by ZIP13 and its implications for spondylocheiro dysplastic Ehlers-Danlos syndrome. Proc Natl Acad Sci U S A 109: E3530–3538. [PubMed: 23213233]

Kim D, Langmead B, and Salzberg SL (2015) HISAT: a fast spliced aligner with low memory requirements. Nat Methods 12: 357–360. [PubMed: 25751142]

Kluska K, Adamczyk J, and Krezel A (2018) Metal binding properties of zinc fingers with a naturally altered metal binding site. Metallomics 10: 248–263. [PubMed: 29230465]

MacDiarmid CW, Taggart J, Kerdsomboon K, Kubisiak M, Panascharoen S, Schelble K, and Eide DJ (2013) Peroxiredoxin chaperone activity is critical for protein homeostasis in zinc-deficient yeast. J Biol Chem 288: 31313–31327. [PubMed: 24022485]

Matsuzawa T, Ohashi T, Hosomi A, Tanaka N, Tohda H, and Takegawa K (2010) The gld1+ gene encoding glycerol dehydrogenase is required for glycerol metabolism in Schizosaccharomyces pombe. Appl Microbiol Biotechnol 87: 715–727. [PubMed: 20396879]

North M, Steffen J, Loguinov AV, Zimmerman GR, Vulpe CD, and Eide DJ (2012) Genome-wide functional profiling identifies genes and processes important for zinc-limited growth of Saccharomyces cerevisiae. PLoS Genet 8: e1002699. [PubMed: 22685415]

Park D, Lee Y, Bhupindersingh G, and Iyer VR (2013) Widespread misinterpretable ChIP-seq bias in yeast. PLoS One 8: e83506. [PubMed: 24349523]

Pavesi G, Mereghetti P, Mauri G, and Pesole G (2004) Weeder Web: discovery of transcription factor binding sites in a set of sequences from co-regulated genes. Nucleic Acids Res 32: W199–203. [PubMed: 15215380]

Peter M, Gartner A, Horecka J, Ammerer G, and Herskowitz I (1993) FAR1 links the signal transduction pathway to the cell cycle machinery in yeast. Cell 73: 747–760. [PubMed: 8500168]

Robinson JT, Thorvaldsdottir H, Winckler W, Guttman M, Lander ES, Getz G, and Mesirov JP (2011) Integrative genomics viewer. Nat Biotechnol 29: 24–26. [PubMed: 21221095]

Ross-Innes CS, Stark R, Teschendorff AE, Holmes KA, Ali HR, Dunning MJ, et al. (2012) Differential oestrogen receptor binding is associated with clinical outcome in breast cancer. Nature 481: 389–393. [PubMed: 22217937]

Sambrook J, and Russell D, (2001) Molecular cloning: a laboratory manual. Cold Spring Harbor Laboratory Press.

Stark R, and Brown GD (2011) DiffBind: differential binding analysis of ChIP-seq peak data. Bioconductor. http://bioconductor.org/packages/release/bioc/vignettes/DiffBind/inst/doc/DiffBind.pdf.

Trapnell C, Hendrickson DG, Sauvageau M, Goff L, Rinn JL, and Pachter L (2013) Differential analysis of gene regulation at transcript resolution with RNA-seq. Nat Biotechnol 31: 46–53. [PubMed: 23222703]

Trapnell C, Roberts A, Goff L, Pertea G, Kim D, Kelley DR, et al. (2012) Differential gene and transcript expression analysis of RNA-seq experiments with TopHat and Cufflinks. Nat Protoc 7: 562–578. [PubMed: 22383036]

Tsai CS, Shi JL, and Ye HG (1995) Kinetic studies of gluconate pathway enzymes from Schizosaccharomyces pombe. Arch Biochem Biophys 316: 163–168. [PubMed: 7840612]

Wang F, Kim BE, Dufner-Beattie J, Petris MJ, Andrews G, and Eide DJ (2004) Acrodermatitis enteropathica mutations affect transport activity, localization and zinc-responsive trafficking of the mouse ZIP4 zinc transporter. Hum Mol Genet 13: 563–571. [PubMed: 14709598]

Wang Y, Weisenhorn E, MacDiarmid CW, Andreini C, Bucci M, Taggart J,et al. (2018) The cellular economy of the Saccharomyces cerevisiae zinc proteome. Metallomics 10: 1755–1776. [PubMed: 30358795]

Wang Z, Feng LS, Matskevich V, Venkataraman K, Parasuram P, and Laity JH (2006) Solution structure of a Zap1 zinc-responsive domain provides insights into metalloregulatory transcriptional repression in Saccharomyces cerevisiae. J Mol Biol 357: 1167–1183. [PubMed: 16483601]

Wilson S, and Bird AJ (2016) Zinc sensing and regulation in yeast model systems. Arch Biochem Biophys 611: 30–36. [PubMed: 26940262]

Wu CY, Bird AJ, Chung LM, Newton MA, Winge DR, and Eide DJ (2008) Differential control of Zap1-regulated genes in response to zinc deficiency in Saccharomyces cerevisiae. BMC Genomics 9: 370. [PubMed: 18673560]

Wu CY, Bird AJ, Winge DR, and Eide DJ (2007) Regulation of the yeast TSA1 peroxiredoxin by ZAP1 is an adaptive response to the oxidative stress of zinc deficiency. J Biol Chem 282: 2184–2195. [PubMed: 17121842]

Wu CY, Roje S, Sandoval FJ, Bird AJ, Winge DR, and Eide DJ (2009) Repression of sulfate assimilation is an adaptive response of yeast to the oxidative stress of zinc deficiency. J Biol Chem 284: 27544–27556. [PubMed: 19656949]

Wu YH, Frey AG, and Eide DJ (2011) Transcriptional regulation of the Zrg17 zinc transporter of the yeast secretory pathway. Biochem J 435: 259–266. [PubMed: 21250939]

Zhao H, Butler E, Rodgers J, Spizzo T, Duesterhoeft S, and Eide D (1998) Regulation of zinc homeostasis in yeast by binding of the ZAP1 transcriptional activator to zinc-responsive promoter elements. J Biol Chem 273: 28713–28720. [PubMed: 9786867]

Zhao H, and Eide D (1996) The yeast ZRT1 gene encodes the zinc transporter protein of a high-affinity uptake system induced by zinc limitation. Proc Natl Acad Sci U S A 93: 2454–2458. [PubMed: 8637895]

Zurlinden A, and Schweingruber ME (1997) Identification of a DNA element in the fission yeast Schizosaccharomyces pombe nmt1 (thi3) promoter involved in thiamine-regulated gene expression. J Bacteriol 179: 5956–5958. [PubMed: 9294459]

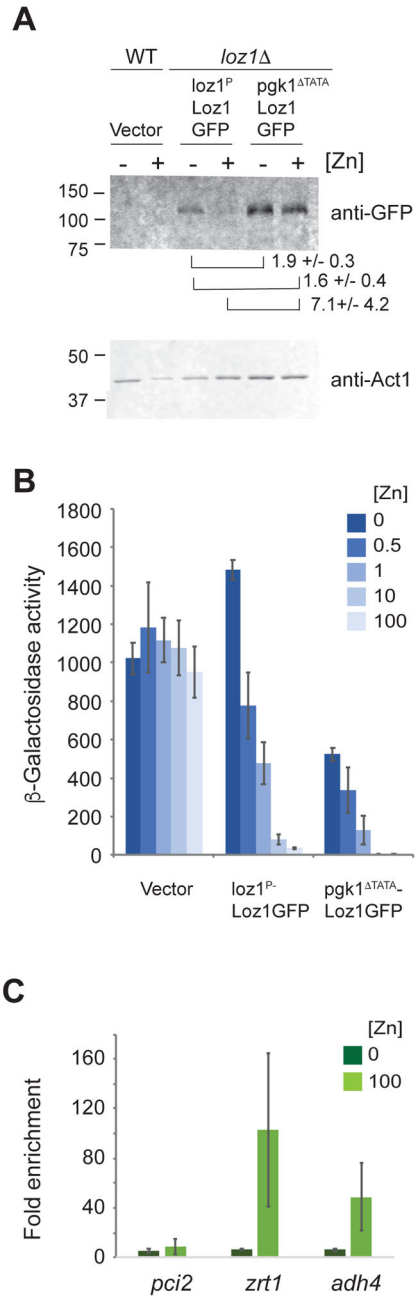

Figure 1.

Generation of a Loz1GFP expression vector for ChIP-seq analysis. A) Immunoblot analysis of crude protein extracts isolated from wild-type cells and *loz1*Δ cells expressing *pgk1*$^{\Delta TATA}$-Loz1GFP or *loz1*^{p}-Loz1GFP following growth overnight in ZL-EMM (-Zn) or in ZL-EMM + 100 μM Zn^{2+} (+Zn). Blots were probed with anti-GFP and anti-Act1 (Actin), which served as a loading control. The positions of the molecular weight markers (in kDa) are indicated on the left. Immunoblots were performed in triplicate and a representative blot is shown. The numbers below the anti-GFP panel indicate the mean increase in *pgk1*$^{\Delta TATA}$-Loz1GFP relative to the *loz1*^{p}-Loz1GFP with +/− standard deviations. *N*=3

(B) β-galactosidase activity was assayed in *loz1*Δ cells co-expressing a *zrt1-lacZ* reporter and the indicated plasmids following growth overnight in ZL-EMM supplemented with 0, 0.5, 1, 10, or 100 μM Zn^{2+}. Data represents the mean values with error bars representing standard deviations. *N*=3

(C) ChIP-qPCR experiments to validate that the *pgk1*$^{\Delta TATA}$-Loz1GFP protein could be used for ChIP analysis. *loz1*Δ cells expressing *pgk1*$^{\Delta TATA}$-Loz1GFP were grown overnight in ZL-EMM with 0 (-Zn) or 100 μM Zn^{2+}(+Zn), and ChIP-qPCR carried out with primers flanking the *zrt1* and *adh4* promoters. The fold enrichment in the immunoprecipitations relative to input DNA was calculated as described in the materials and methods. Primers specific to the *psi2* promoter were used as a negative control. The numbers are the average fold enrichment with error bars showing standard deviations. *N*=3

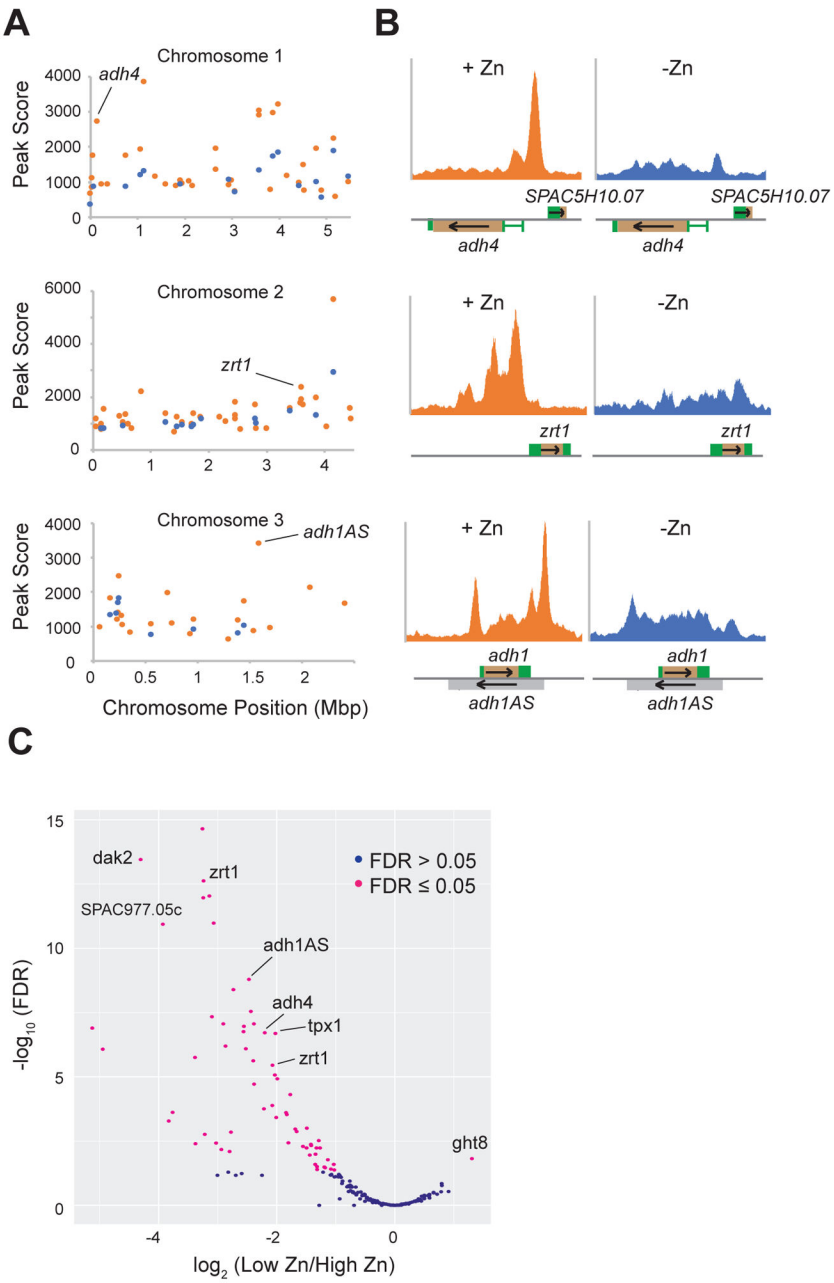

Figure 2.

Identification of Loz1 binding sites using ChIP-seq (A) ChIP-seq was performed as described in the materials and methods. The input-normalized fold enrichment profiles for peaks enriched in high zinc (orange dots) and low zinc (blue dots) were plotted against chromosome position. Positions of peaks in the promoters of characterized Loz1 target genes *adh4*, *zrt1*, and *adh1AS* are indicated.

(B) ChIP-seq data was visualized with the Integrative Genomics Viewer Software. Snapshots of the peaks identified in the *adh4*, *zrt1*, and *adh1AS* promoters in low and high zinc are shown.

(C) Volcano plot of the confidence scores of Loz1 binding sites plotted against the zinc-dependent fold-change in normalized read counts. Loz1 binding sites where there is a greater than 2-fold increase in binding under one condition (low zinc or high zinc) as compared to the other, have been colored pink.

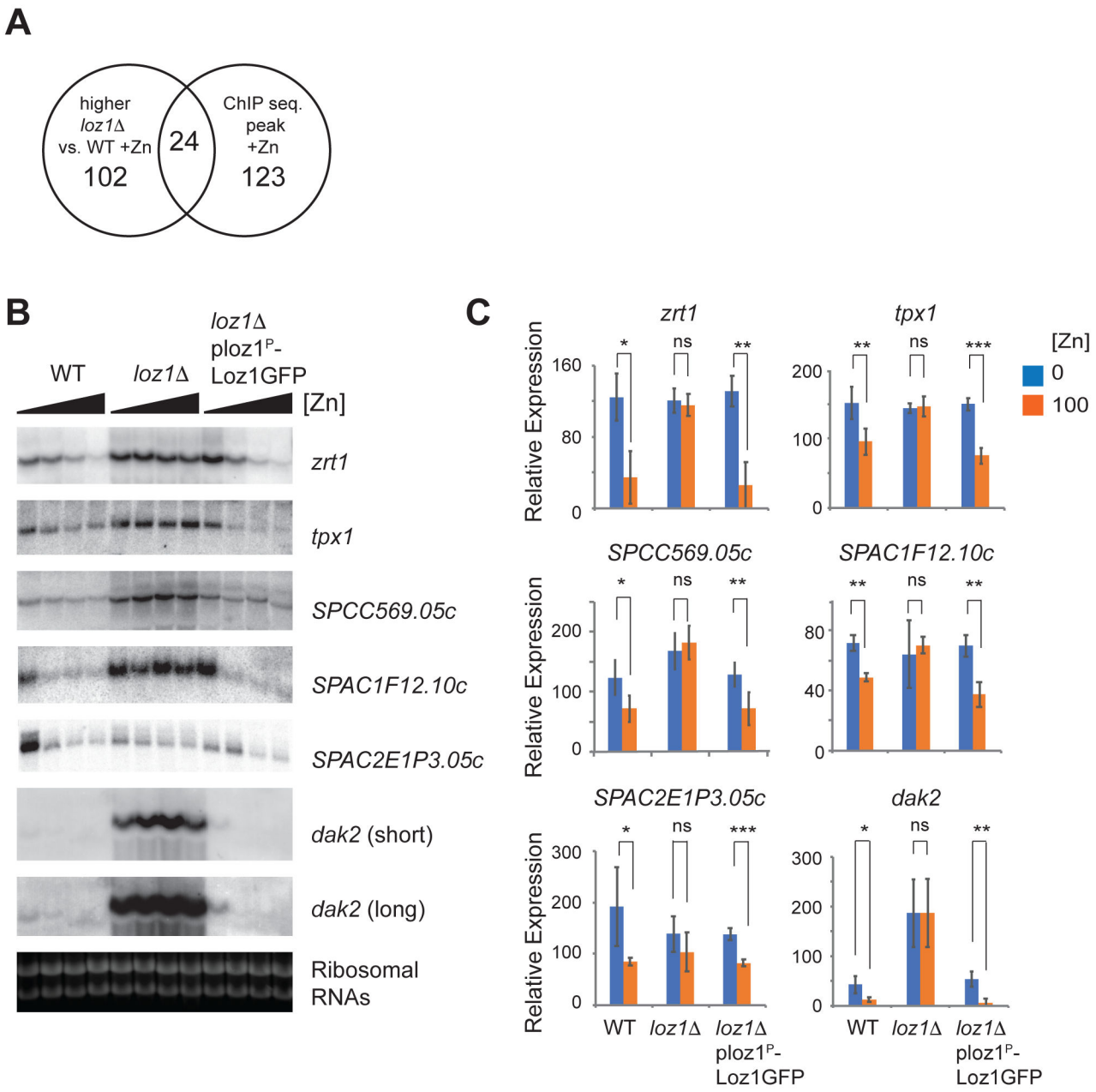

Figure 3.

Identification of genes that are repressed by Loz1 in high zinc conditions A) Venn diagram representing the overlap of genes expressed at a higher level in *loz1*Δ cells grown in high zinc, and protein coding genes that contain a Loz1 ChIP-seq peak within 1500 bp of the transcriptional start site following growth in zinc-replete conditions. When ChIP-seq peaks were located in the promoters of two divergently transcribed genes (49 of 98 peaks), both genes were included.

B) To validate results from the RNA-seq analysis the indicated strains were grown overnight in ZL-EMM supplemented with 0, 1,10,100 μM Zn. Total RNA was prepared from the indicated strains and subjected to RNA blot hybridization with the indicated probes. A

representative blot is shown on the left. Ribosomal RNAs were used as the loading control, and *zrt1* representing a previously characterized Loz1 target gene. Due to the differences in *dak2* transcript abundance in wild-type and *loz1*Δ cells, short and long exposures are shown. C) Quantification of RNA blot analysis. Hybridization signals obtained with the indicated P32 labelled probes were detected by phosphorimaging and were quantitated using Image J. The values were normalized to the 18 S rRNA and represent the average value of 3–4 independent replicates. Error bars represent +/− standard deviations and p values were determined using a student's t-test. ***p<0.001, **p<0.01, *p<0.05, ns not significant.

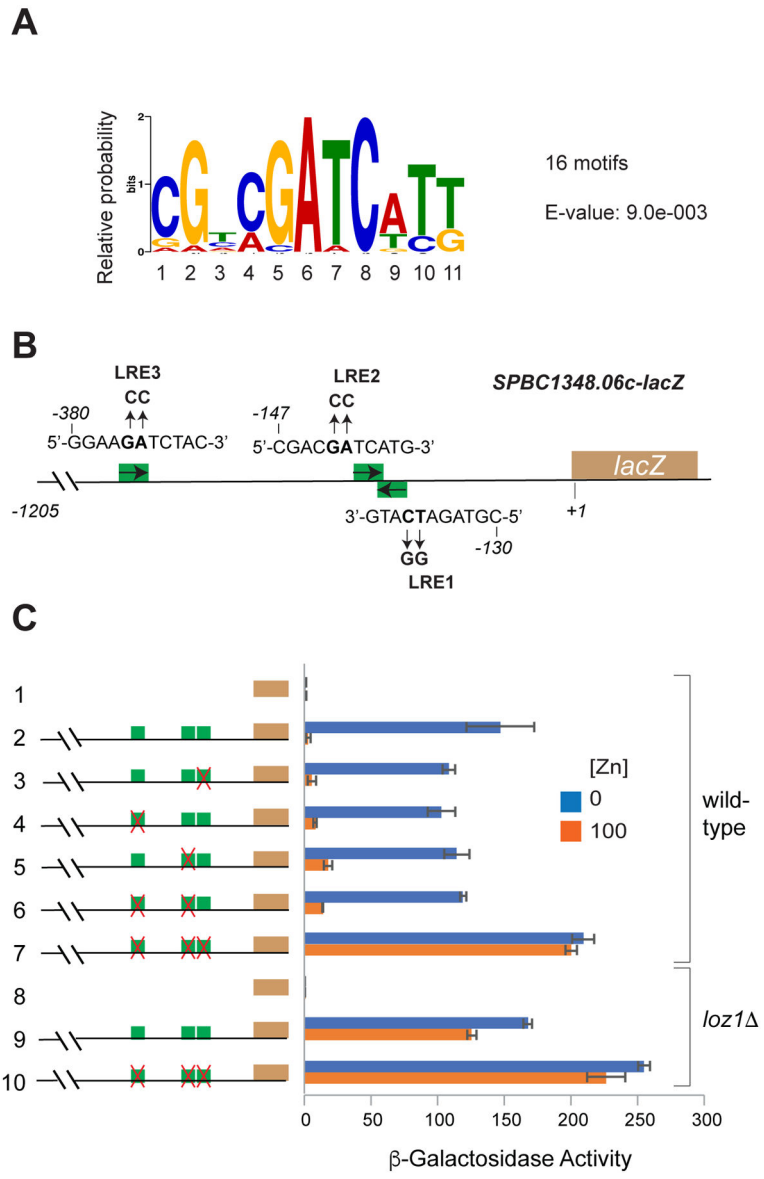

Figure 4.

The Loz1 response element is required for Loz1-mediated gene repression. A) The program MEME was used to identify putative cis-acting DNA elements that were located in the promoters of Loz1 target genes. The shown motif (named the Loz1 response element) was enriched in ChIP-seq peaks of genes that were repressed by Loz1 in high zinc.

B) A schematic diagram of the *SPBC1348.06c-lacZ* reporter highlighting the positions and sequences of putative LREs. The numbers indicate the distance of the first base of the motif to the putative ATG initiation codon. Nucleotide substitutions that were introduced to disrupt LRE function are shown in bold.

C) Wild-type or *loz1*Δ cells expressing the indicated *SPBC1348.06c-lacZ* reporter genes were grown overnight in ZL-EMM supplemented with 0 or 100 μM zinc before cells were harvested and assayed for β-galactosidase activity. The relative positions of the putative LREs in the reporters are indicated by green boxes. The positions of mutated LREs are

shown by green boxes with red crosses. Data represents the mean values with error bars representing standard deviations. *N*=3

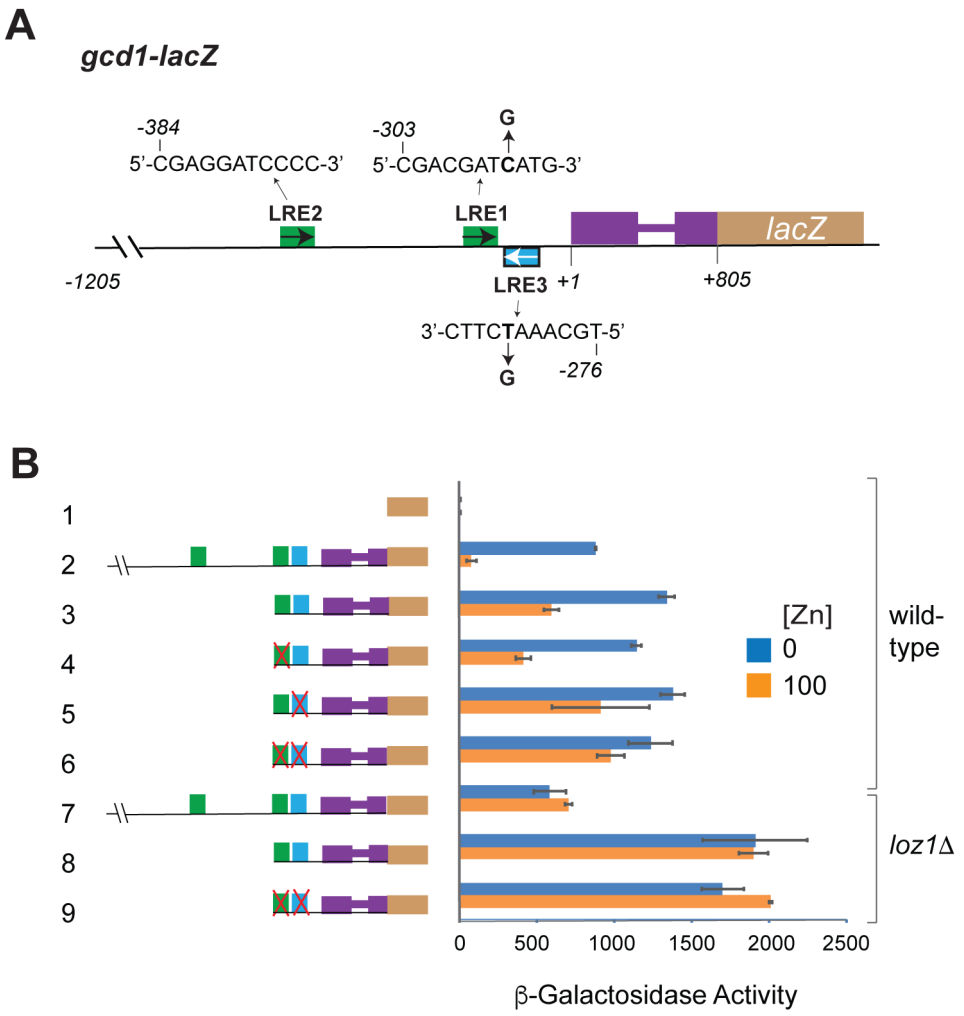

Figure 5.

Loz1-dependent repression of the *gcd1* promoter is dependent upon multiple LREs A) A schematic diagram of the *gcd1-lacZ* reporter highlighting the positions and sequences of putative LREs (green and blue boxes) and the position of the *gcd1* 5'UTR (purple boxes and line). The numbers indicate the distance of the first base of each motif relative to the putative transcriptional start site for *gcd1*. Nucleotide substitutions that were introduced to disrupt LRE function are shown in bold.

B) Wild-type or *loz1*Δ cells expressing the indicated *gcd1-lacZ* reporter genes were grown overnight in ZL-EMM supplemented with 0 or 100 μM zinc before cells were harvested and assayed for β-galactosidase activity. The relative positions of the putative LREs in the reporters are indicated by green and blue boxes. The positions of mutated LREs are shown by green and blue boxes with red crosses. Numbers represent the average value with error bars representing standard deviations. *N*=3

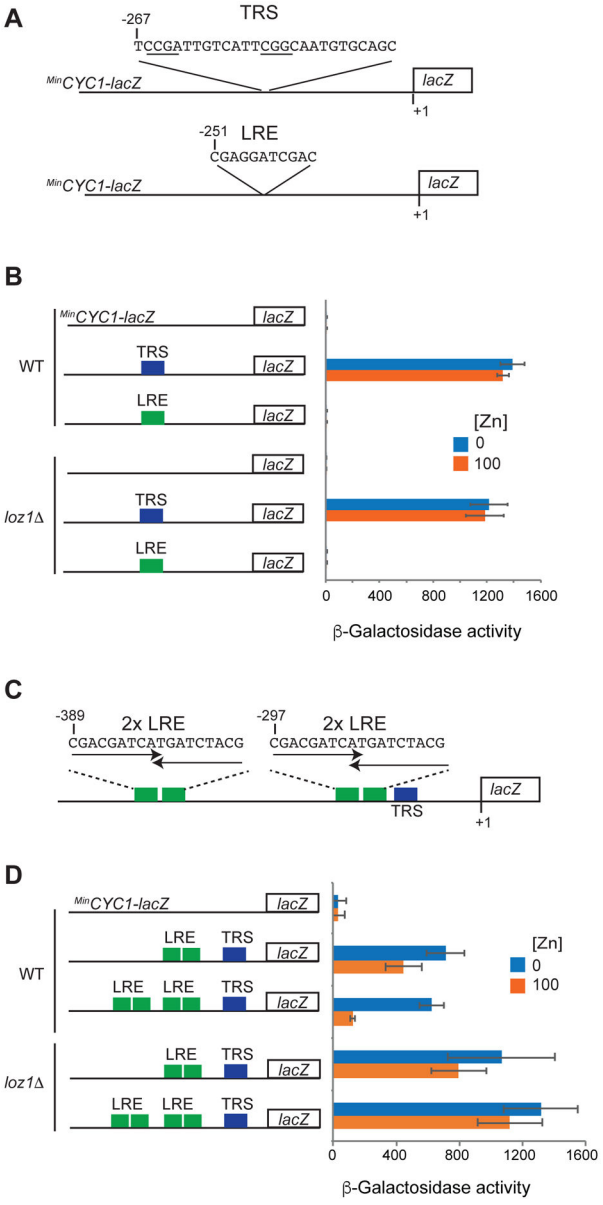

Figure 6.

The LRE is sufficient for Loz1-mediated gene repression.A) A schematic diagram of the *Min*CYC1-lacZ reporter containing a thiamine responsive element (TRS) or LRE. The numbers indicate the distance of the first base of the motif to the putative ATG initiation codon.

B) Wild-type or *loz1*Δ cells expressing the indicated *Min*CYC1-lacZ reporter gene were grown overnight in ZL-EMM supplemented with 0 or 100 μM zinc before cells were harvested and assayed for β-galactosidase activity. Numbers represent the average value with error bars representing standard deviations. *N*=3

C) A schematic diagram of the *Min*CYC1-lacZ reporter containing the TRS and 2 copies of LRE1 and LRE2 from the *SPBC1348.06c-lacZ* reporter. The numbers indicate the distance of the first base of the motif to the putative ATG initiation codon.

D) Wild-type or *loz1*Δ cells expressing the indicated ^{Min}*CYC1-lacZ* reporter gene were grown overnight in ZL-EMM supplemented with 0 or 100 μM zinc before cells were harvested and assayed for β-galactosidase activity. Numbers represent the average value with error bars representing standard deviations. *N*=3.

Table 1.
Loz1 target genes that were identified by RNA-seq and ChIP-seq.

Gene	Common Name	Function[i]	RNA-seq Δ*loz1*/WT +Zn Fold increase Log2 (average)	Putative LRE Sequence	Position[†]	Loz1-Dependent regulation[‡]
Transmembrane transport						
SPAC977.17		MIP water channel	7.40	TGCAGATCCCG	−970	
				TGCAGATCCAA	−993	
SPBC16D10.06	*zrt1*	Plasma membrane ZIP zinc transmembrane transporter	5.16	AGCAGATCCTT	−735	(Corkins *et al.*, 2013, Ehrensberger *et al.*, 2014)
				TGACGATCGAA	−1515	
SPCC548.07c[$]	*ght1*	Plasma membrane high −affinity glucose:proton symporter	4.70	GGAAAATCCAA	−1766	
				TGGCAATCCCC	−1808	
				TGCAAATCGCC	−1817	
SPCC1529.01[$]		Transmembrane transporter	3.48	GGAAAATCCAA	−1281	
				TGGCAATCCCC	−1239	
				TGCAAATCGCC	−1230	
SPCC569.05c		Spermidine family transporter	2.84	CGTAGATCATG	−639	This study
SPBC1683.08	*ght4*	Plasma membrane hexose:proton symporter	1.92	GGACGATCTCC	−959	
				CGGAGATCGTC	−980	
				TGAAGATCGAT	−1056	
SPAC4H3.01		DNAJ domain protein Caj1/Djp1 type	1.39	CGTCGATCATT	−1321	
				TGCCGATCACT	−1339	
Carbohydrate metabolic processes						
SPAC977.16c	*dak2*	Dihydroxyacetone kinase	8.61	TGCAGATCCAA	+530	This study
				CGGGATCTGCA	+497	
SPCC13B11.02c	*adh1AS*	Adh1 antisense transcript	7.99	CGTCGATCATT	−295	(Corkins *et al.*, 2013)
				CGGCGATCCAT	−106	
				TGCCGATCAGA	−163	
				AGAAGATCAAA	−185	
				TGATGATCAAA	−207	
SPAC5H10.06c	*adh4*	Alcohol dehydrogenase	6.80	CGACGATCACG	−917	(Corkins *et al.*, 2013, Ehrensberger *et al.*, 2014)
				AGAAGATCTTG	−953	
				AGAAGATCCAC	−954	
				CGTGGATCTTC	−965	
				TGTGGATCACT	−981	
SPCC794.01c	*gcd1*	Glucose dehydrogenase	6.30	GGATGATCGAA	−816	(Corkins *et al.*, 2017)
SPAC4F8.07c	*hxk2*	Hexokinase 2	1.08	AGTCGATCGAC	−1870	

Gene	Common Name	Function[Ï]	RNA-seq Δ*loz1*/WT +Zn Fold increase Log2 (average)	Putative LRE Sequence	Position[†]	Loz1-Dependent regulation[‡]
				CGTCGATCGAC	−1859	
Gene Regulation and signaling						
SPAC25B8.19C	*loz1*	Zinc−responsive transcription factor	3.01	CGCAGATCATT	−1397	(Corkins *et al.*, 2013)
				CGTCGATCATA	−1386	
				CGCCGATCACC	−1075	
SPAC57A10.05c	*pof1*	F−box/WD repeat protein	1.39	CGTAGATCATT	−750	
				TGCAGATCAGT	−855	
SPAC19D5.01[¶]	*pyp2*	Tyrosine phosphatase	1.46	CGAGGATCAGA	−882	
SPAC4G8.03c	*puf5*	Pumilio family RNA −binding protein mRNA metabolic process	1.38	AGTCGATCTTG	−2728	
Unknown/pombe specific						
SPBC1348.06c[§] (*SPBPB2B2.15 SPAC977.05c*)		Velum formation protein	11.07	CGTAGATCATG	−130	(Corkins *et al.*, 2013)
				CGACGATCATG	−147	
				GGAAGATCTAC	−380	
SPAC57A10.06	*mug15*		4.95	CGTAGATCATT	−954	
				TGCAGATCAGT	−859	
SPBC12C2.14c		dubious	3.76	CGTCGATCTTT	−692	
				CGCAGATCTTT	+75	
				CGTCGATCCTG	+188	
				CGTCGATCTTG	+158	
				TGTCGATCACG	+149	
				TGGTGATCCAA	+113	
SPBC660.05[¶]			3.06	GGAAGATCATA	−606	
SPAC5H10.07			2.51	CGACGATCACG	−599	
				AGAAGATCTTG	−563	
				AGAAGATCCAC	−562	
				CGTGGATCTTC	−551	
				TGTGGATCACT	−535	
SPAC2E1P3.05c[¶]		Fungal cellulose binding domain protein	1.82	AGTCGATCCTG	−141	This study
Other						
SPAC1F12.10c		NADPH−hemoprotein reductase	2.02	CGTCGATCATT	−229	This study
				TGCCGATCACT	−211	
SPCC576.03c	*tpx1*	thioredoxin peroxidase unfolded protein binding	1.54	CGCCGATCATT	−194	This study
				TGCAGATCCTG	−156	
SPCC11E10.01[$]		Cystathionine beta−lyase	1.37	AGCTAATCATA	−989	

Gene	Common Name	Function[Ї]	RNA-seq Δ*loz1*/WT +Zn Fold increase Log2 (average)	Putative LRE Sequence	Position[†]	Loz1-Dependent regulation[‡]
SPBC12C2.03c		Methionine synthase reductase	1.18	CGCAGATCTTT	−1648	
				CGTCGATCCTG	−1761	
				CGTCGATCTTG	−1731	
				TGTCGATCACG	−1722	
				TGGTGATCCAA	−1696	
				CGTCGATCTTT	−882	
SPCC757.12		Alpha−amylase homolog	1.04	GGCCGATCGCT	−702	

[†]Numbers represent the position of the LRE relative to the putative translational ATG codon, with the exception of the *adh1AS* transcript. For this ncRNA the number represents the distance of the LRE relative to the previously mapped transcriptional start in low zinc conditions (Ehrensberger *et al.*, 2013).

[‡]Genes where Loz1-dependent regulation has been confirmed independently by RNA blot or *lacZ*-reporter gene analysis, in this study or in other reports.

[§]These genes were grouped together because SPBC1348.06c shares 100% and ≥99% identity SPBPB2B2.15 and SPAC977.05c at the mRNA level, respectively. The sequence of the LREs and surrounding regions are also identical for these genes.

[¶]Genes where the putative LRE sequence was found with the region surrounding the peak detected in the ChIP-seq analysis

[$]Genes that did not contain a NGNNGATCNNN sequence in the Loz1 ChIP seq. peak or surrounding region. These ChIP-seq peaks contained NGNNAATCNNN sequences, which are shown in gray text.

[Ї]Functional categories were assigned based on GO term annotations obtained from PomBase GO tool analysis (Lock et al., 2018, The Gene Ontology, 2019).